Journal of Alloys and Compounds 513 (2012) 495–498

Contents lists available at SciVerse ScienceDirect

Journal of Alloys and Compounds

journal homepage: www.elsevier.com/locate/jallcom

Switchable mirror based on Mg–Zr–H thin films

Shanhu Bao[a,b], Yasusei Yamada[b], Kazuki Tajima[b], Ping Jin[a,b], Masahisa Okada[b], Kazuki Yoshimura[b,*]

[a] Research Center for Industrial Ceramics, Shanghai Institute of Ceramics, Chinese Academy of Science, 215 Chengbei Road, Jiading District, Shanghai 201800, China
[b] Materials Research Institute for Sustainable Development, National Institute of Advanced Industrial Science and Technology (AIST), 2266-98 Shimoshidami, Moriyama-ku, Nagoya 463-8560, Japan

ARTICLE INFO

Article history:
Received 30 March 2011
Received in revised form 15 October 2011
Accepted 29 October 2011
Available online 7 November 2011

Keywords:
Switchable mirror
Mg–Zr thin film
Hydriding and dehydriding
Metal hydrides
Gasochromic materials
Hydrogen storage alloy

ABSTRACT

A Mg–Zr thin film is prepared on a glass substrate by co-sputtering of Mg and Zr targets and *in situ* sputtering of a thin Pd overlayer. The structural and optical properties of Mg–Zr and Mg–Zr–H thin film are investigated induced by hydrogen absorption and/or desorption at room temperature. Optical transmission and reflection data indicated that Mg–Zr–H thin film is the color-neutral in the visible range with chromaticity coordinates of $x = 0.3566$ and $y = 0.3430$. The formation of the ternary hydride $Mg_{0.82}Zr_{0.18}H_2$ is confirmed in an Mg-rich Mg–Zr solid solution thin film in the hydride state. The hydrogen insertion and extraction occurs in fcc lattice structure. Because the volume change according to hydrogenation and dehydrogenation, the switching durability is much better than that of the switchable mirror using Mg–Ni alloy.

1. Introduction

Mg based alloy materials have attracted much attention as hydrogen storage materials [1], hydrogen sensors [2], and optical switches [3,4]. The Mg based alloy thin films with a thin Pd top layer show reversible optical change due to the hydrogenation and dehydrogenation at room temperature [3]. In recent years, a number of ternary hydrides of magnesium based alloy have been synthesized by heating powder mixtures of MgH_2 and together with MH_2 (M = Mn, Cr, Ti, V, Nb, Ta, Zr, and Hf) at high pressure [5–11]. These magnesium based alloys show the high hydrogen capacity (3–5.5 wt%) and the reversible hydrogen absorbing and desorbing characterizations. These materials also can be used as a 'switchable mirror', which is a new kind of optical switching material and is switched between transparent and mirror states by hydrogenation and dehydrogenation of thin film [12–14]. We studied Mg_yTiH_x and Mg_yNbH_x thin films with a thin Pd top-layer as a switchable mirror and reported that they show good optical switching properties.

Recently, the fully hydrogenated face-centered cubic (fcc) phase of Mg–Zr–H ($Mg_{0.82}Zr_{0.18}H_2$ ($a \approx 4.87$ Å)) [6,15] was synthesized. Its hydrogen capacity is 5.3 wt%. The fcc Mg–Zr–H phase exhibits reversible hydrogen loading and unloading properties under high pressure of 0.1–0.5 MPa, and shows the highly stability compare to other hydrides of Mg–M (M = Ti, V, Nb, Ta) series [7–9], which is very important when it is used as a switchable mirror. We pay attention to this hydride of Mg–Zr–H in the search as a new switchable mirror material.

In this paper, we prepared Mg–Zr thin films with a thin Pd top layer on the glass substrate by sputtering and their gasochromic switching properties have been investigated using diluted hydrogen gas.

2. Experimental procedures

Mg–Zr alloy thin films are deposited by DC magnetron cosputtering of Mg (99.99%) and Zr (99.99%) targets on glass substrates at room temperature. Pd cap layer, which is a catalyst and a protection layer against the oxidization of Mg, is subsequently deposited on Mg–Zr layer *in situ* condition. The base pressure is 2.0×10^{-5} Pa, and the target-to-substrate distance is 15 cm. The sputtering power to Mg and Zr targets is set at 30 W and 15–40 W, respectively, with the process pressure of 1.0 Pa (Ar flow rate of 20 sccm). The power of Pd overlayer is set at 30 W and the process pressure is 1.6 Pa.

Thin film thicknesses are measured with a stylus profilometer (Kosaka ET-350). The composition of the $Mg_{(1-x)}Zr_x$ thin films deposited on Si substrates is investigated by Rutherford backscattering spectrometry (RBS). The crystalline structure of Pd-capped Mg–Zr and Mg–Zr–H thin films is investigated by X-ray diffraction (XRD) measurement using a thin film X-ray diffractometer (Cu-Kα, λ = 1.5418 Å, Rigaku XRD system). The morphologies of Mg–Zr alloys before and after hydrogenation are characterized by a scanning electron microscopy (SEM).

The characterization setup of optical switching is described in detail elsewhere [16]. Gasochromic switching is performed by loading of 4% hydrogen in argon gas at room temperature. The optical change is monitored by the combined use of a laser diode (λ = 670 nm) and a Si photodiode. The duration of gas loading is 30 s, followed by 300 s unloading. Optical transmission and reflection spectra of Mg–Zr alloys

* Corresponding author. Tel.: +81 52 736 7305; fax: +81 52 736 7406.
E-mail address: k.yoshimura@aist.go.jp (K. Yoshimura).

0925-8388/$ – see front matter © 2011 Elsevier B.V. All rights reserved.
doi:10.1016/j.jallcom.2011.10.098

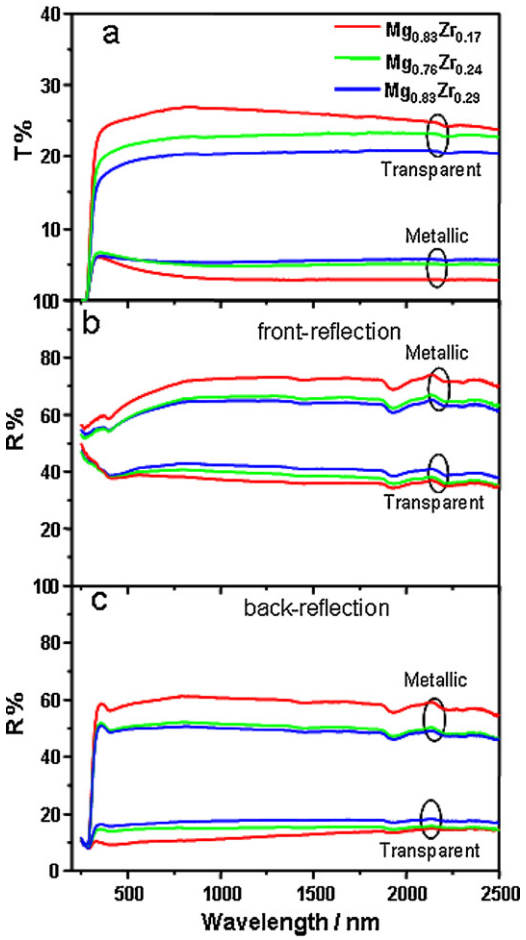

Fig. 1. Vis-near infrared transmittance and reflectance spectra of 40 nm $Mg_{(1-x)}Zr_x$ (x = 0.17, 0.24, 0.29) films with 4 nm Pd top layers on glass substrates in hydride and metallic states.

before and after hydrogenation are recorded using a UV–Vis–NIR optical photometer (JASCO V570) in the wave length range from 300 to 2500 nm.

3. Results and discussions

3.1. Optical properties of metallic and hydride thin film

We prepared Mg–Zr thin films with three different components $Mg_{(1-x)}Zr_x$ (x = 0.17, 0.24, and 0.29). The thickness of Mg–Zr layer and Pd layer is 40 nm and 4 nm, respectively. All as-deposited samples have shiny metallic surface. After exposure to hydrogen containing atmosphere, it shows drastic change into a transparent state by hydrogenation of Mg–Zr layer.

The transmittance and reflectance spectra for obtained samples are shown in Fig. 1. The transmittance in the transparent state is measured by filling the specimen holder with 4% hydrogen in Ar. The reflectance spectra are measured both from the back side (substrate side) and the front side (thin film side) of the deposited film. In the metallic state, the Pd/$Mg_{(1-x)}Zr_x$ sample show a reflectance around 50% (back side) and 60% (front side), and a transmittance is around 5%. In the hydride state, the transmittance increases above 20% and the reflectance decrease around 15% (back side) and 40% (front side) with increasing Zr content, while the reflectance is increasing. The transmittance in the transparent state increases with increasing the Zr content in Mg–Zr alloy. The front side reflectance is high in both of metallic and hydride states compared with that of the back side reflectance. The difference of reflectance from back and front sides comes from the difference of the refractive index variation between Pd and Mg–Zr layer and that between Mg–Zr layer and glass substrate.

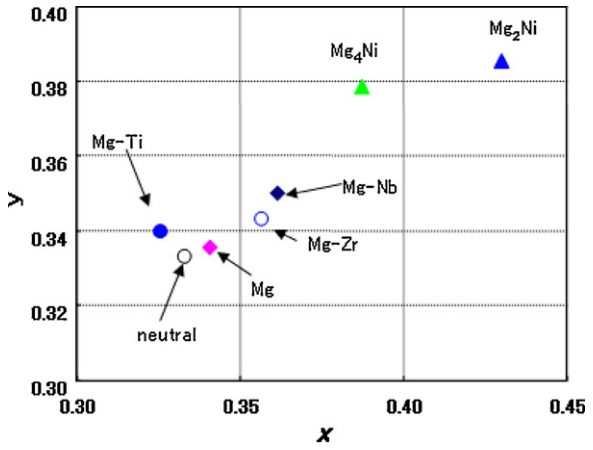

Fig. 2. XYZ colorimetric system xy chromaticity diagram for the Mg based switchable mirror systems.

The fully hydrogenated films look almost colorless. The chromaticity coordinates of Mg–Zr sample in the transparent state are x = 0.357 and y = 0.343, which are calculated from the transmittance spectrum in the hydride state (Fig. 2). The color neutrality of the $Mg_{(1-x)}Zr_x$ mirror is markedly higher than that of the Mg–Ni switchable mirror which looks slightly yellowish in the hydride state [3,17] and almost comparable to that of Mg–Ti and Mg–Nb. This color neutrality of the Mg–Zr thin film is an advantage for application of smart window. However, the transmission modulation of Mg–Zr mirror is small and its transmission is reduced by increasing the Zr content.

3.2. The microstructures of Mg–Zr alloy and Mg–Zr–H hydride

The crystalline structures of the as-deposited and hydrogenated samples are investigated by XRD measurement. Fig. 3 shows the XRD patterns of the Pd-capped $Mg_{(1-x)}Zr_x$ alloy thin films. Thickness of the Mg–Zr and Pd layers are 90 nm and 4 nm, respectively. Red lines are for as-deposited samples. A strong diffraction peak is seen at $2\theta = 34.8^\circ$ in as-deposited films of Mg–Zr. In the case of Mg–Ti and Mg–Nb thin films, we have reported that their peak positions are shifted to a higher angle direction with an increasing of Ti ($2\theta = 38.52^\circ$ (0 0 2), hexagonal structure) or Nb ($2\theta = 38.55^\circ$ (1 1 0), cubic structure) content in Mg–M (M = Ti, Nb) thin films according to Vegard's low. However, the peak position does not shift with varying of Mg/Zr ratio in this case. That is because the atomic radius of Mg and Zr is very close; 0.150 nm for Mg and 0.155 for Zr, respectively [18]. The peak position of 34.8° is between the Mg (34.4°, 0 0 2) and Zr (34.83°, 0 0 2). A broad diffraction peak of Pd also have found at centered of 40°.

3.3. The hydrogenation and dehydrogenation kinetics of Mg–Zr alloy

Fig. 4 shows the hydrogenation and dehydrogenation kinetics of $Mg_{(1-x)}Zr_x$ (x = 0.17, 0.24, 0.29) thin films upon 4% hydrogen gas loading and unloading at room temperature. The transmission modulation versus loading time is measured at 670 nm wavelength when hydrogenation and dehydrogenation. The hydrogenation speed is not affected by Zr content, which can be achieved in the transparent state within 3–5 s. The maximum transmittance has strong dependence on Zr content in the $Mg_{(1-x)}Zr_x$ thin films. $Mg_{0.83}Zr_{0.17}$ shows large optical modulation and it decreases with

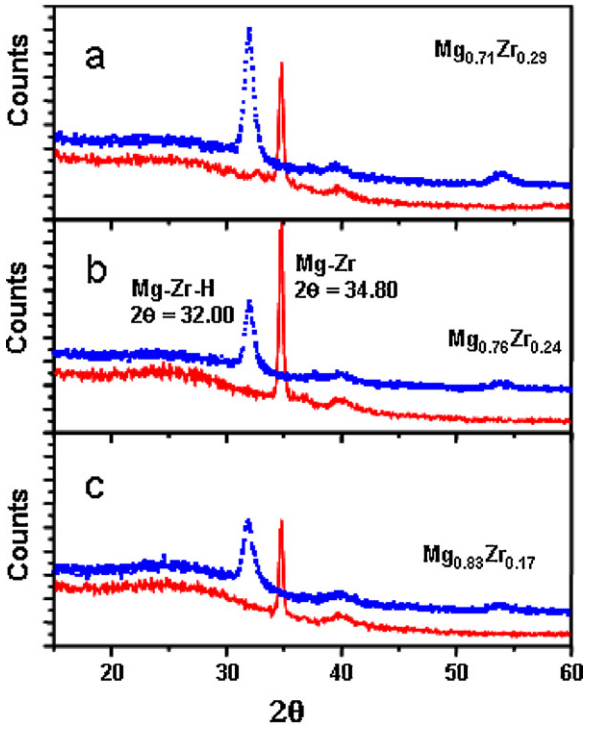

Fig. 3. X-ray diffraction spectra of 90 nm $Mg_{(1-x)}Zr_x$ (x = 0.17, 0.24, 0.29) thin films top covered with 4 nm Pd layer. (Solid line) as-deposited samples, (dot line) *in situ* measured of hydrogenation samples with 4% hydrogen gas loading.

increasing of Zr content. However, the dehydrogenation speed is much slower than that of other samples.

To investigate the mechanism of switching of Mg–Zr thin film, the crystalline structure of the samples in the hydride state is also characterized by *in situ* XRD measurement (Fig. 5). The specimen chamber of the diffractometer is filled with 4% H_2 in Ar during the measurement. Fig. 5 shows the XRD patterns of 90 nm thick $Mg_{76}Zr_{0.24}$ thin film in as-deposited, hydrogenated and dehydrogenated states. After hydrogenation, we found the diffraction peak of $2\theta = 34.75^\circ$ have disappeared for $Mg_{(1-x)}Zr_x$ (x = 0.17, 0.24, and 0.29) samples. And the newly diffraction peaks appears at $2\theta = 31.65^\circ$ (strong) and 54.05° (weak) The peak position of these diffraction peaks coincide with the reported values for new ternary hydride of $Mg_{0.82}Zr_{0.18}H_2$ phase synthesized in a GPa hydrogen pressure methods [6,15]. $Mg_{0.82}Zr_{0.18}H_2$ phase has fcc structure.

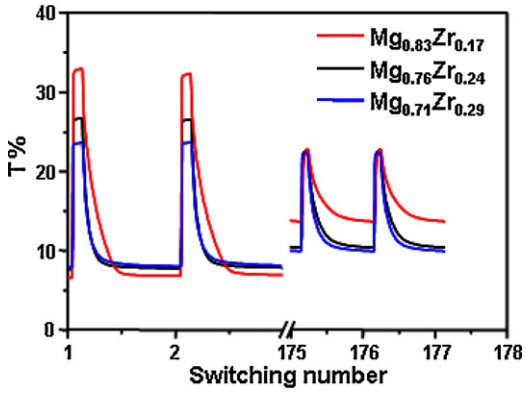

Fig. 4. Hydrization and dehydrization kinetics of 40 nm $Mg_{(1-x)}Zr_x$ (x = 0.17, 0.24, 0.29) thin films with a 4 nm Pd overlayer. Transmission modulation is measured at 670 nm wavelength upon hydrogen gas loading. The duration of gas loading is 30 s, followed by 300 s unloading.

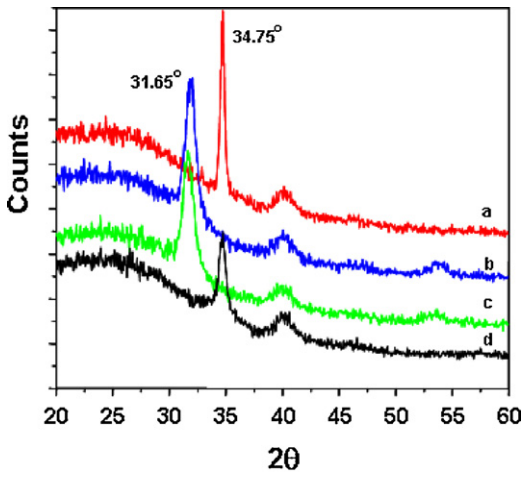

Fig. 5. XRD patterns of 90 nm $Mg_{76}Zr_{0.24}$ thin film; (a) Mg–Zr film as-deposited metallic state, (b) Mg–Zr–H hydride state, (c) Mg–Zr film after dehydrogenated, (d) Mg–Zr film after dehydrogenated for 6 days.

It indicates that $Mg_{0.82}Zr_{0.18}H_2$ is formed in Mg–Zr thin films upon hydrogen gas loading.

By exposure to air, the hydrogenated sample goes back to the metal state. We found that Pd/Mg–Zr samples show a characteristic behavior at this dehydrogenation process, which has been not observed for Mg–Ti or Mg–Nb switchable mirror thin films. After dehydrogenation, the transmittance goes back to the metallic state, as shown in Fig. 4. However, Fig. 5 indicates that the lattice structure remains to fcc after dehydrogenation and it does not goes back to hcp structure. The result means that the optical switching of Mg–Zr switchable mirror occurs by insertion and extraction of hydrogen in fcc lattice. In the case of Mg–Ni, lattice structure is changed between

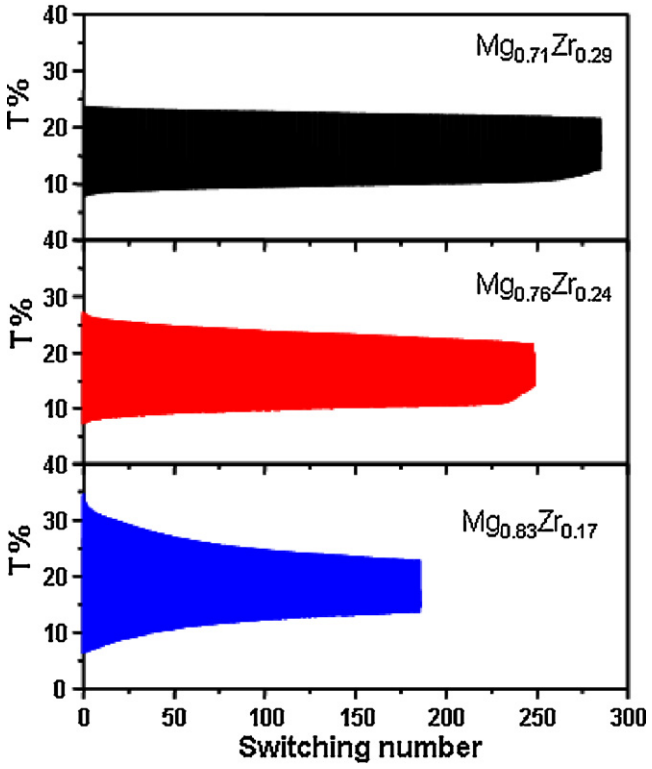

Fig. 6. Comparison of switching durability of 40 nm $Mg_{(1-x)}Zr_x$ (x = 0.17, 0.24, 0.29) switchable mirror thin films with a 4 nm Pd overlayer. Other condition is same as Fig. 5.

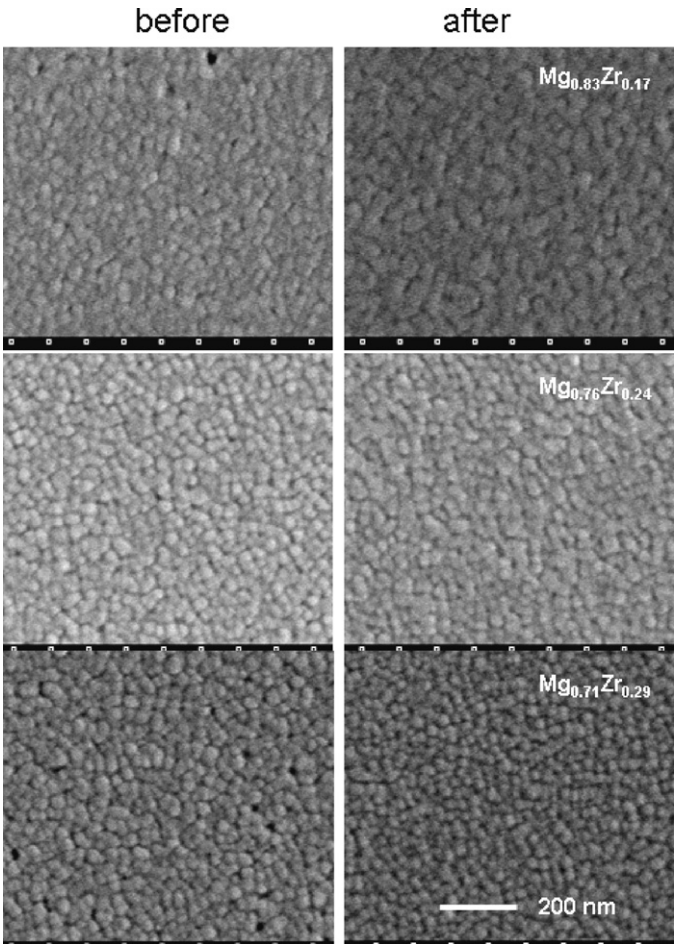

Fig. 7. SEM image of 40 nm $Mg_{(1-x)}Zr_x$ (x = 0.17, 0.24, 0.29) thin films with a 4 nm Pd overlayer before and after hydrogenation.

the metallic and hydride states. The black line in Fig. 5(d) is XRD pattern of the sample which is kept in air in the transparent state after 6 days. The lattice structure returns to the initial hcp state. It implies that the hydrogen extracted fcc structure is not stable and it is gradually transformed to hcp structure in oxygen containing atmosphere. It means that the dehydrogenate state is not the stable state.

3.4. Switching lifetime for Mg–Zr thin film

Next we tested the switching durability. Fig. 6 shows the optical change by gasochromic switching after long term switching for the samples of $Mg_{(1-x)}Zr_x$ (x = 0.17, 0.24, 0.29). The switching sequence is the same as Fig. 4. Although $Mg_{0.83}Zr_{0.17}$ has wide optical modulation range initially, the modulation level shrinks fast. The switching durability increases with increasing of Zr content. $Mg_{0.83}Zr_{0.17}$ sample can be switched even after 250 switching cycles, which is much longer than that of Mg–Ni thin film [19]. Such better switching durability comes from the above mentioned unique switching mechanism. In the case of Mg–Ni, Mg–Ti and Mg–Nb, large volume change accompanies hydrogenation and dehydrogenation, which damages the uppermost Pd layer [19]. But in the case of Mg–Zr, the volume change is small and the accompanied damage may be suppressed.

In the case of Mg–Ni, degradation is caused by the damage of outermost Pd layer. To compare, we observe the surface morphology of the Mg–Zr sample after long term gasochromic switching. Fig. 7 shows the FE-SEM surface image of $Mg_{(1-x)}Zr_x$ (x = 0.17, 0.24, and 0.29) samples before and after hydrogen gas loading. As shown in Fig. 7, the surface of Mg–Zr thin film before hydrogen gas loading is very similar to Mg–Ti [12] and Mg–Nb [13] thin films, that is consisted with particle of the form of island. This tendency is clear with increase of the content of Zr. This characterization is different form Mg–Ni alloy thin film prepared at same sputtering conditions, which shows no such structure of island form in Mg–Ni [19] alloy thin film before hydrogen gas loading. The most striking point is that almost no damage structure is observed for the surface of the degraded samples. In the case of Mg–Ni, the surface of Pd/Mg–Ni sample was highly damaged [19].

These results show that Mg–Zr is a promising material for practical use of switchable mirror from the view point of switching durability.

4. Conclusion

In conclusion, Pd-capped Mg–Zr thin films are prepared by DC magnetron sputtering. $Mg_{(1-x)}Zr_x$ (x = 0.29, 0.24, 0.17) with a 4 nm Pd cap layer shows an excellent optical switching properties by alternate exposure to 4% H_2 in Ar gas and air. Pd/Mg–Zr thin films are color neutral in the hydride (transparent) state, which an advantage in smart window applications. The formation of the ternary hydride $Mg_{0.82}Zr_{0.18}H_2$ is confirmed in an Mg-rich Mg–Zr solid solution thin film in the hydride state. The hydrogen insertion and extraction occurs in fcc lattice structure. Because the volume change according to hydrogenation and dehydrogenation, the switching durability is much better than that of the switchable mirror using Mg–Ni alloy.

Acknowledgment

The authors acknowledges the special funding support from the National Natural Science Foundation of China (NSFC No. 51032008).

References

[1] J.J. Reilly, R.H. Wiswall, Inorg. Chem. 7 (1968) 2254.
[2] K. Yoshimura, M. Okada, M. Tazawa, P. Jin, Trans. Mater. Res. Soc. J. 27 (2002) 365.
[3] T.J. Richardson, J.L. Slack, R.D. Armitage, R. Kostecki, B. Farangis, M.D. Rubin, Appl. Phys. Lett. 78 (2001) 3047.
[4] D.M. Borsa, R. Fremaud, A. Baldi, H. Schreuders, J.H. Rector, B. Kooi, P. Vermeulen, P.H.L. Notten, B. Dam, R. Griessen, Phys. Rev. B 75 (2007) 205408.
[5] D. Moser, D.J. Bull, T. Sato, D. Noreus, D. Kyoi, T. Sakai, N. Kitamura, H. Yusa, T. Taniguchi, W.P. Kalisvaart, P. Notten, J. Mater. Chem. 19 (2009) 8150–8161.
[6] D. Kyoi, T. Sakai, N. Kitamura, A. Ueda, S. Tanase, J. Alloys Compd. 463 (1-2) (2008) 311–316.
[7] T. Sato, D. Kyoi, E. Ronnebro, N. Kitamura, T. Sakai, D. Noreus, J. Alloys Compd. 417 (1-2) (2006) 230–234.
[8] D. Kyoi, T. Sato, E. Ronnebro, N. Kitamura, A. Ueda, M. Ito, S. Katsuyama, S. Hara, D. Noreus, T. Sakai, J. Alloys Compd. 372 (1-2) (2004) 213–217.
[9] D. Kyoi, T. Sato, E. Ronnebro, Y. Tsuji, N. Kitamura, A. Ueda, M. Ito, S. Katsuyama, S. Hara, D. Noreus, T. Sakai, J. Alloys Compd. 375 (1-2) (2004) 253–258.
[10] H. Blomqvist, E. Ronnebro, D. Kyoi, T. Sakai, D. Noreus, J. Alloys Compd. 358 (1-2) (2003) 82–86.
[11] D. Kyoi, E. Ronnebro, N. Kitamura, A. Ueda, M. Ito, S. Katsuyama, T. Sakai, J. Alloys Compd. 361 (1-2) (2003) 252–256.
[12] S. Bao, K. Tajiama, Y. Yamada, M. Okada, K. Yoshimura, Appl. Phys. A 87 (2007) 621–624.
[13] S. Bao, K. Tajiama, Y. Yamada, P. Jin, M. Okada, K. Yoshimura, J. Ceram. Soc. Jpn. 116 (2008) 771–775.
[14] S. Bao, K. Tajiama, Y. Yamada, M. Okada, K. Yoshimura, Sol. Energy Mater. Sol. Cells 92 (2008) 224–227.
[15] T. Takasaki, D. Kyoi, N. Kitamura, S. Tanase, T. Sakai, J. Phys. Chem. B 111 (51) (2007) 14102–14106.
[16] K. Yoshimura, S. Bao, Y. Yamada, M. Okada, Vacuum 80 (2006) 684.
[17] K. Yoshimura, Y. Yamada, M. Yasusei, Appl. Phys. Lett. 81 (2002) 4709.
[18] J.C. Slater, J. Chem. Phys. 41 (1964) 3199.
[19] K. Yoshimura, Y. Yamada, S. Bao, K. Tajima, M. Okada, Jpn. J. Appl. Phys. 46 (2007) 4260–4264.